Polymer(Korea), Vol. 30, No. 2, pp 124-128, 2006

# 레이더 흡수특성이 있는 저적외선 방출 복합섬유의 제조 및 특성 연구

**Bin Yu and Lu Qi**†

*Research Institute of Biological and Spinning Materials, Tianjin Polytechnic University, 63 Chenglin Road, Hedong District, Tianjin 300160, China*

(2005년 10월 24일 접수, 2006년 3월 10일 채택)

# Preparation and Characterization of Low Infrared Emissivity Bicomponent Fibers with Radar Absorbing Property

**Bin Yu and Lu Qi**†

*Research Institute of Biological and Spinning Materials, Tianjin Polytechnic University, 63 Chenglin Road, Hedong District, Tianjin 300160, China*

*(Received October 24, 2005;accepted March 10, 2006)*

**Abstract :** Heavy weight of the camouflage materials was always the main problem. To solve it, the low infrared emissivity fibers with the radar absorbing property (LIFR) were prepared. The low infrared emissivity fibers (LIF) were firstly melt-spun by co-extrusion of polypropylene (PP) and PP/various fillers master-batches using general conjugate spinning. The infrared emissivity of LIF with Al and ZnO was decreased respectively compared with that of pure polypropylene fibers. The infrared emissivity of LIF with 15 wt% Al and 2 wt% ZnO in the sheath-part can reach 0.58. To improve LIF radar absorbing property, LIFR was prepared by filling the 50 wt% ferrite and bronze in the core-part of LIF. The radar absorbing efficacy of LIFR was good and the infrared emissivity was low. For the characterization, fiber electron intensity instrument and differential scanning calorimetry (DSC) were used for the analysis of mechanical properties, thermal and crystallization behavior of the spun-fibers. Scanning electron microscopy (SEM) was carried out to observe the particle distribution of the bicomponent fibers.

**Keywords :** fibers, polypropylene, low infrared emissivity, radar absorbing.

## Introduction

Infrared camouflage technology has become more and more important with the development of radar stealth technology, electronic warfare, and high-mobility of modern fighters.[1] Infrared camouflage technologies include cooling, shield, cover and low infrared emissivity coating, etc. to eliminate or reduce the temperature difference between objects and background, to reduce the infrared radiation intensity and brightness of objects, and to restrict the infrared radiation direction of objects.[2-8] However, the infrared camouflage paint coating materials are base one at present, heavy weight of the material being still a concerning problem. To remedy this problem, more and more research about infrared camouflage materials has been concentrated on fiber materials.[9,10] In addition, radar and infrared technology are major and universal technology in military reconnaissance and control and guide now. Single functional infrared camouflage materials can't realize the concealment against infrared and radar target surveillance sensor devices simultaneity. Existing researches on infrared-radar camouflage materials are focused on the multi-layer coating materials.[11-13] But the coat materials have many defects such as thicker coat, great density and weight and so on.

To solve the problem, we studied how to design an organic-inorganic bicomponent fiber in this paper, which will display low infrared emissivity with the radar absorbing properties. For this purpose, we have prepared sheath-core type fibers using PP chips and different concentration of fillers.

## Experimental

**Materials.** The aluminium (Al) particles with 4 μm particle size provided from Angang Group Aluminium Powder Co., Ltd. China and nanometer zinc oxide (ZnO) with 50 nm mean diameter supplied by Beijing Central Iron & Steel Research Institute, China were filled into the sheath-part for low infrared emissivity. The ferrite supplied by Beijing Central Iron & Steel Research Institute and rich bronze powder from Wuxi Gold Powder Factaroy, China were used as radar absorbing agents in the core-part with the mean diameter of 3 μm. Polypropylene chips (isotactic PP) were provided from Shanghai Petrochemical Co. Ltd, China. Its characteristics commonly used for fibers spinning are as follows: $M_n$ : $1.7\times10^5$, MI: 39.0 g/10 min, density: 0.92 g/cm$^3$, and polydispersity : 3.8. For easier spinning process, PP/fillers master-batches were prepared by a conventional twin-screw

†To whom correspondence should be addressed.
E-mail: yubin7712@163.com

extruder.

**Spinning Process.** The spinning machine was a general conjugate spinning machine which was composed of two extruders ($L/D$=25, $D$=20 mm) and gear pumps. Both PP chips and PP/fillers master-batches were dried for at least 2 hrs at 100 ℃ in vacuum drier to secure complete moisture-free state. The PP/Al, PP/ZnO and PP/Al/ZnO master-batches were added in the sheath-section respectively and the PP chips were added in the core-section for the preparation of the LIF. The LIFR was prepared by input the ferrite and rich bronze in the core-section of the LIF. Sheath-core ratio of the fibers was 40/60 (W/W) controlled through adjustment of the speed of gear pumps. Two kinds of master-batches were melted in both cylinders, combined in the spinneret. They were extruded through the mono-nozzles, which have diameter of 0.4 $\Phi$mm.

Figure 1 illustrates the spinning system used for generating sheath- core bicomponent fibers. The processing temperatures are listed in Table 1.

**Thermal Analysis.** For thermodynamic experiment, dynamic scanning calorimerer (DSC, Perkin-Elmer DSC-7) equipped with a cooler was used under the nitrogen atmosphere. All the samples were heated from 0 to 250 ℃ at 10 ℃/min. From this procedure, apparent enthalpies of fusion were calculated from the area of the endothermic peak. The percent crystallinity of polypropylene was evaluated using the following equation:

$$\text{crystallinity}(\%) = \frac{\Delta H_f}{\Delta H_f^0 \cdot \omega_f}$$

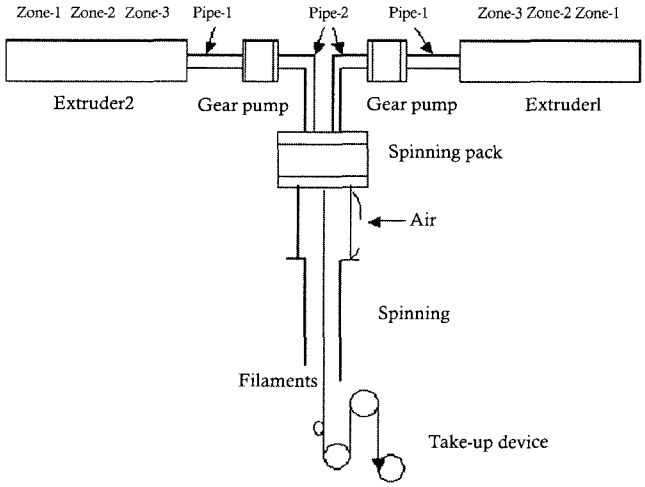


**Figure 1.** Schematic diagram for the bicomponent fibers spinning system.

**Table 1. Processing Temperature(℃) for Generating Sheath-Core Bicomponent Fibers (Refer to Figure 1 for Illustration)**

| | Pack | Pipe-2 | Gear pump | Pipe-1 | Clamp | Zone-3 | Zone-2 | Zone-1 |
|---|---|---|---|---|---|---|---|---|
| Temperature (℃) | 255 | 250 | 240 | 240 | 240 | 240 | 240 | 150 |

where $\Delta H_f$ is the heat of fusion of PP fibers, $\omega_f$ is the weight fraction of PP in the blends, and $\Delta H_f^0$ is the extrapolated value of the enthalpy corresponding to the heat of fusion of 100% crystalline PP taken as 209 kJ/kg from the literature.[14]

**Morphology Observation.** The cross-section structure of the sheath-core bicomponent fibers were observed using scanning electron microscope (SEM, Hitachi 450 and Quanta 200). The SEM samples were goldsputtered before observation.

**Performance Test of Infrared Emissivity of the Fibers.** The infrared emissivity was measured with 5DX Fourier infrared spectroscopic instrument (NICOLET, America) and black-body oven (JD-1, Jilin University, China ) at 100 ℃ ,wavelengths from 5 to 25 μm.

**The Test of the Mechanical Properties of the Fibers.** The mechanical properties of the fibers were tested by fiber electron intensity apparatus (YG003A, Changzhou Textile Instrument Factory, China) with the descendent velocity of 5 mm/min, and 200 g pre-strain. The breaking elongation $\alpha = l_1 - l_0 / l_0 \times 100\%$, where $l_1$ is the breaking length and $l_0$ is 10 mm.

**Performance Test of Radar Absorbing of the Fibers.** The performance of radar absorbing was evaluated by reflectivity using Arch Method. Reflectivity $R$ is ratio of the materials reflective power to metallic plate reflective power on which the materials were placed, which can be expressed as:

$$R = \frac{P_a}{P_m}$$

where $P_a$ is the reflective power of the sample and $P_m$ is the reflective power of the metallic plate.

In practice, we surveyed the ratio of the reflective power of the sample and the reflective power of metallic plate to a same reference signal that was in direct proportion to the transmission signal respectively.

$$R_m = \frac{P_m}{P_i}, \quad R_a = \frac{P_a}{P_i}$$

Where $P_i$ is reference signal. So

$$R = \frac{P_a}{P_m} = \frac{P_a / P_i}{P_m / P_i} = \frac{R_a}{R_m}$$

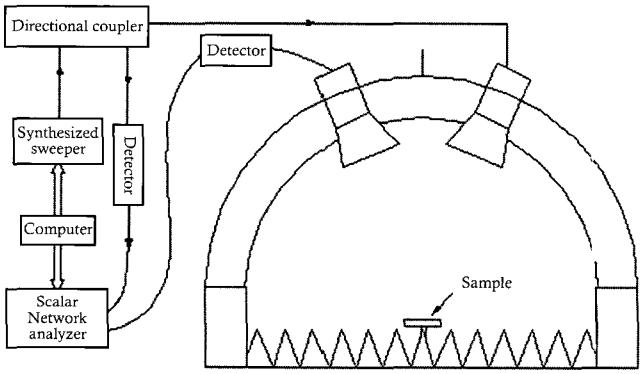


**Figure 2.** Reflectivity measurement setup of arch method.

The reflectivity was finally expressed with db as:

$$R_{db} = 10\lg R_a - 10\lg R_m$$

The schematic diagram of the experimental setup is shown in Figure 2. The reflectivity of the samples were measured and compared with that from a plane metallic plate. Measurement was carried out using an HP 8757E network analyzer in the sweep frequency range from 2 to 18 GHz. All samples were made 180×180 $mm^2$ in order to cover the metallic plate.

## Results and Discussion

**Thermal Property.** Differential scanning calorimetry thermograms and the variation of PP crystallinity of all the LIF are depicted in Figures 3 and 4. Figures 3(a) and 3(b) show the curves of the DSC thermogram profile of LIF containing micrometre Al particles and nanometer ZnO respectively in the sheath-part. In DSC graphs, crystallinity of fibers containing micron particles in the sheath-part increased slightly at first and then decreased as the filler content rose (Figure 4(a)). The reason may be that a small quantity of the particle was acted as nucleating agents and internal plasticizer which make for the regular arrangement of macromolecular at low particle content. It resulted in the increase

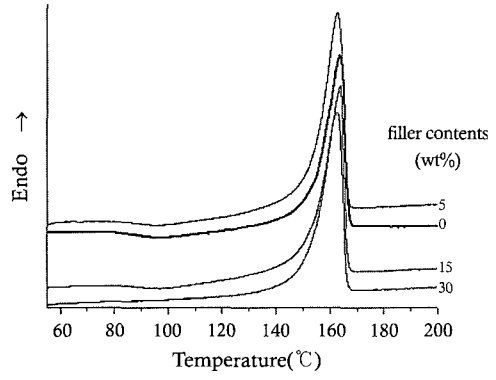


**Figure 3.** The DSC curves of the LIF with the micrometer Al particle (a) and the nanometer ZnO (b) in the sheath-part respectively.

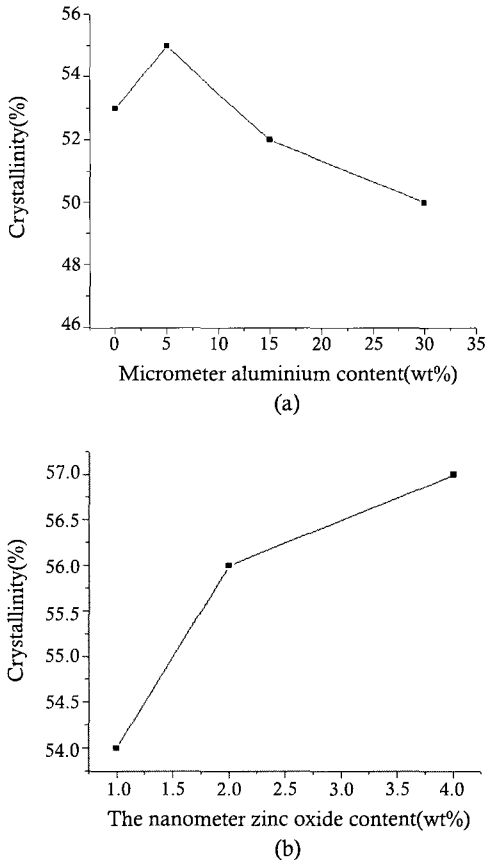


**Figure 4.** The variation of crystallinity of the LIF having (a) Al particle and (b) ZnO in sheath-part respectively.

of crystallinity of fibers. However, with the filler content increase, many particles will baffle the movement of the macromolecular as the impurities and affect the growth of crystal which leaded to the decrease of the crystallinity. The wt% crystallinity of PP was calculated via the standard heat of crystallization which was taken to be 209 J/g. Recently, Yeo[15] *et al.* reported that the addition of nanometer silver made the crystallinity of fibers reduce. However, in the case of our results, the behavior of PP crystallization in the matrix led to a different result (Figure 4(b)). The increase in crystallinity of PP revealed that the nanoparticles accelerate the crystallization of PP. Thus we supposed that nanoparticles in the PP matrix acted as a nucleating agent.

**Cross-sections of Fibers Observation.** SEM is a good way to present a real-space image of the particles filled in the polymer materials. Hence, the cross-section of the fibers was observed on SEM. In Figure 5, SEM micrograph shows the cross-sections of LIF sheath-part filled with 15 wt% Al particles (Figure 5(a)) and 30 wt% Al particles(Figure 5(b)). In Figure 5(b), some conglomerations of the particles and holes were observed. The SEM photograph of sheath-part filled with 15 wt% particles had a few conglomeration and hole in Figure 5(a). It was demonstrated that the compatibility of the PP with the particles became bad with the particle content increase which will affect the mechanical properties of the fibers sometimes.

The Figure 6 shows the cross-section of the LIFR with 15 wt% Al in

sheath-part and 50 wt% ferrite and bronze particles in the core-part. The obvious core-sheath structure was observed and there were seldom configuration disfigurement in the Figure 6. This image indicates that spinnability of materials of core-part and sheath-part are good for bi-component fibers.

**The Mechanical Properties.** Tables 2 and 3 indicate the mechanical property of the LIF with the Al and ZnO particles. In this result, the breaking elongation and breaking stress of the fiber including Al decreased with the microparticles content increase. But the breaking stress of the fibers with the ZnO nanoparticles was raised with the increasing ZnO content. The reduction in mechanical property of the fiber with Al particles was considered that the increase of interface of polymer and microparticles interfered with the mechanical properties of the fiber. The increase in the breaking stress of the fiber with ZnO was explained by the cross-linking of macromolecule of PP by nanoparticles and the crystallinity increase (Figure 4(b)).

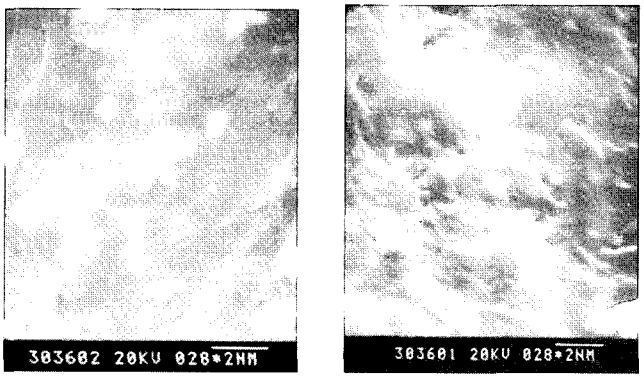


**Figure 5.** SEM photographs (×5.00 k) of the sheath-part with Al. (a) 15 wt% and (b) 30 wt% .

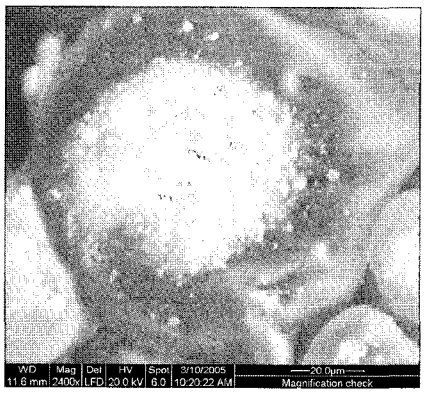

**Figure 6.** The cross-section of the LIFR with 15 wt% Al in the sheath-part and 50 wt% ferrite and rich bronze in the core-part.

**Table 2. The Effect of the Al Content in the Sheath-Part on the LIF Mechanical Properties**

| The Al particles content(wt%) | 5 | 15 | 30 |
|---|---|---|---|
| Breaking elongation(%) | 85 | 60 | 42 |
| Breaking stress(CN/dtex) | 5.45 | 4.89 | 4.18 |

**Table 3. Mechanical Properties of Fibers with the Nanometer ZnO**

| The Al nanoparticles content(wt%) | 1 | 2 | 4 |
|---|---|---|---|
| Breaking elongation(%) | 90 | 80 | 75 |
| Breaking stress(CN/dtex) | 5.73 | 6.59 | 6.69 |

**The Infrared Emissivity and the Radar Absorption Property.** The low infrared emissivity materials are mainly obtained by mixing of the resin with metal particle.[6,7] The Al is used widely in the low infrared emissivity materials owing to its low price. In recent research,[8] some nanometer particle was added into the resin to reduce the emissivity of the materials. However, little attention is played on researching the effect of Al/nanoparticles on the materials. So in the present research, we investigated the emissivity of the LIF with Al, nanometer ZnO and Al/ZnO. Figures 7 and 8 indicate the infrared emissivity curves of the LIF with Al and ZnO. The results showed that the input of the Al particles made the infrared emissivity of the fiber fall sharply and the infrared emissivity reached the lowest value when the Al content was 15 wt%. The input of single ZnO also made the infrared emissivity of the fibers decrease. Since the fiber with 15 wt% Al obtained the lowest infrared emissivity,

We studied the effect of ZnO on the infrared emissivity of fiber with

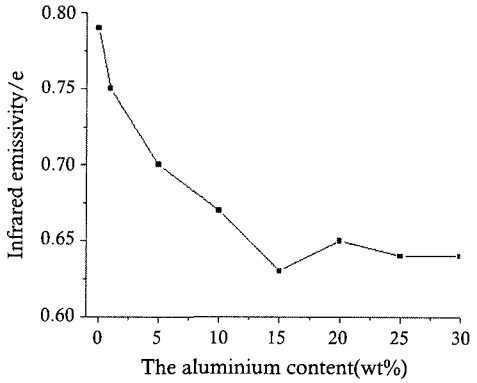


**Figure 7.** The change of infrared emissivity of the LIF with the Al paiticles content increase.

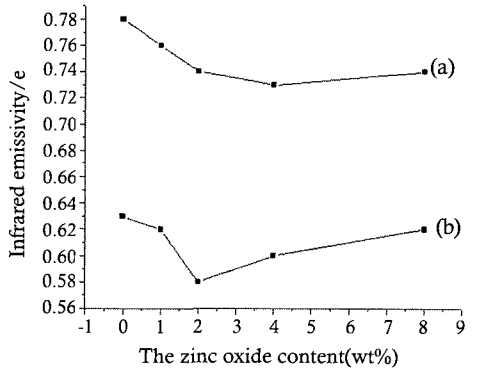


**Figure 8.** The effect of the ZnO content on the infrared emissivity of the LIF. (a) The fiber without Al and (b) the fiber with 15 wt% Al in the sheath-part.

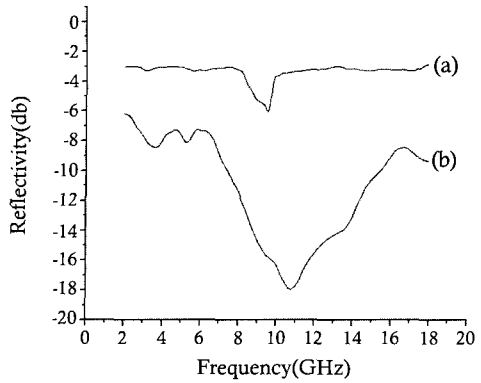


**Figure 9.** The reflectivity curves of the LIF and LIFR. (a) LIF with 15 wt% Al and 2 wt% ZnO and (b) LIFR with 15 wt% Al and 2 wt% ZnO in the sheath-part and 50 wt% ferrite and rich bronze in the core-part.

15 wt% Al (Figure 8, line 2). The research indicated that ZnO can reduce the infrared emissivity of the fiber with the constant Al content 15 wt%. As we all known, the sum of absorptivity and reflectivity is 1, for the opacity materials. According to the Kirchoff's Law, absorptivity is in direct ratio to emissivity. So the emissivity is inverse ratio to the reflectivity. The reflectivity of Al is very high which means the low emissivity. So Al can adjust the infrared emissivity of PP. But there were some conglomerations of the particles with the Al content rise (Figure 5) that made the reflectivity decrease and emissivity increase, and even affected the mechanical properties of the fiber sometimes. Furthermore, the increase in metal content made against the radar absorbing. So the 15 wt% is the optimal content in the sheath-part of fiber. The reduction of the infrared emissivity of the fiber with ZnO only was considered that the surface effect and micro-dimension effect of the nanoparticles improve the reflectivity. On the other hand, there sometimes are crystal lattice aberrances among the ZnO crystal, as the Lu has reported,[8] which may produce the infrared. So its infrared emissivity did not always decrease. When the ZnO nanoparticles were inputed into the sheath-part with the 15 wt% Al, the infrared emissivity of fiber was reduced a little. The Al cooperation with the nanometer ZnO can explain that. It is well-known that the Rayleigh scattering happens when an incident electromagnetic wave with the wavelength far smaller than the particles size impinges on the smaller particles. The ZnO particle size was about 50 nm while the infrared wavelength from 5~25 μm. So the Rayleigh scattering was going to happen when the infrared impinged on the ZnO particles. The widespread and almost isotropic Rayleigh scattering waves were impinged on the metal particles which will increase the infrared reflectivity resulting in the infrared emissivity decrease. But too many nanometer particles will produce too many Rayleigh scattering making the infrared emissivity increase. In a word, both of single Al and ZnO can reduce the emissivity of the fiber. The fiber containing the Al/ZnO have reasonable lowest infrared emissivity.

The radar absorption property of the LIFR with 15 wt% Al and 2 wt% ZnO in the sheath-part and 50 wt% ferrite and rich bronze in the core-pate compared with that of the LIF with 15 wt% Al and 2 wt% ZnO in the sheath-part were shown in Figure 9. The results showed that the least reflectivity of the fibers was -17.97db at 10.64 GHz, and 10db absorption bandwidth was 8.01 GHz. But the radar absorbing property of LIF was very poor. The good radar absorbing property of LIFR may because the increase in the increasing magnetic loss and electric loss caused by the addition of bronze and ferrite particles. The research also found the infrared emisssivity of the LIFR can reach 0.60 which is greater than that of the LIF. The input of ferrite with higher emissivity should explain the increase in infrared emissivity of the LIFR. But there was a very limited increase in infrared emissivity of the LIFR compared with that of LIF from 0.58 to 0.60 which can be contributed to the adding of the bronze of low emissivity bronze. So the fiber may become a multi-functional camouflage material with high potential of development and commercial value in the future.

## Conclusions

The sheath-core bicomponent fibers were melt-spun by co-extrusion of PP and PP/various particles master-batches. DSC results showed crystallinity of the spun fibers added the Al particles in the sheath-part slightly increased, then decreased with the content increase which reduced the mechanical properties of the fiber. But the input of ZnO nanoparticles made the crystallinity of the fiber increase and can improve the mechanical properties of the fiber. SEM results showed that inorganic particles in fibers have relatively good dispersibility. The infrared emissivity of LIF containing Al particles and ZnO nanoparticles respectively was decreased compared with that of pure PP fibers. The infrared emissivity of fiber with 15 wt% Al particles and 2 wt% ZnO in the sheath-part can reach 0.58. The radar absorbing efficacy of this LIBR filled with the 50 wt% radar absorbing agents in the core-part was good and the infrared emissivity of the LIFR can reach 0.60.

## References

1. S. M. Burkinshaw, G. Hallas, and A. D. Towns, *Rev. Progr. Coloration Relat. Topics*, **26**, 47 (1996).
2. L Sample, *New Sci.*, **172**, 21 (2001).
3. B. Bernd, *Proc. SPIE Int. Soc. Opt. Eng.*, **3062**, 340 (1997).
4. S. Cudzilo, *Propellants. Explos.. Pyrotech.*, **1**, 12 (2001).
5. M. Vaullerin, P. Morand, and A. Espagnacq, *Propellants. Explos. Pyrotech.*, **5**, 229 (2001).
6. Sutter, U. S. Patent 6,468,647 (2002).
7. R. F. Supcoe, US Paetent 4,311,623 (1982).
8. X. R. Lu, *J. Nanjing Univ. Aeronautics and Astronauticsv(China)*, **5**, 464 (2003).
9. I. Hiroshi and M. Yoshitaka, JP Patent 2003155641 (2003).
10. K. K. Gupta, *J. Ind. Text.*, **31**, 27 (2001).
11. G. James, *Eng. Techn.*, **7**, 16 (2004).
12. G. A. Rao and S. P. Mahulikar, *Aeronaut. J.*, **106**, 629 (2002).
13. W. Bechtold and A. Wenger, CH Patent 692761 (2002).
14. J. Brandrup, E. H. Immergut, and E. A. Grulke, *Polymer Handbook*, John Wiley & Sons Inc., New York, 1999.
15. S. H. Yeo, H. J. Lee, and S. H. Geong, *J. Mater. Sci.*, **38**, 2143 (2002).